

Optical wave properties of nano-particle chains coupled with a metal surface

Vitaliy Lomakin^{1#}, Meng Lu^{2#}, and Eric Michielssen³

¹Department of Electrical and Computer Engineering, University of California, San Diego

²Department of Electrical and Computer Engineering, University of Illinois at Urbana Champaign

³Department of Electrical Engineering and Computer Science, University of Michigan, Ann Arbor
vitaliy@ece.ucsd.edu

Abstract: Optical phenomena supported by ordered and disordered chains of metal nano-particles on a metal surface are investigated by considering a particular example of gold nano-bumps on a gold surface. The TWs supported by these structures are analyzed by studying the frequency-wavenumber spectra of the fields excited by localized sources placed near the chain. Periodic nano-bump chains support traveling waves (TWs) that propagate without radiation loss along, and are confined to the region near, the chain. These TWs are slow waves with respect to both space fields and surface plasmon polaritons supported by the metal surface. For nearly resonant nano-bumps, the TWs are well confined and can be excited efficiently by a localized source placed near the chain but the TW propagation length is short. For non-resonant nano-bumps, the TWs have large propagation lengths but are not well confined and are excited less efficiently. The TWs supported by nano-bump chains were shown to have larger propagation lengths than free-standing chains of the same dimension/size and cross-sectional confinement. TWs also are supported by disordered chains and chains with sharp bends. Perturbations in nano-bump positions are shown to reduce the TW propagation length much less significantly than perturbations in their sizes. Transmission through sharp chain bends is much stronger for nearly resonant nano-bumps than for nonresonant ones. In addition to their ability to support TWs, nano-bump chains can be used to manipulate (excite/reflect/refract) SPPs on the metal surface.

©2007 Optical Society of America

OCIS codes: (160.4670) Optical Materials, (310.6860) Thin Films, Optical Properties

References and Links

1. C. Bohren and D. Huffman, *Absorption and Scattering of Light by Small Particles* (J. Wiley New York, 1983).
2. J. R. Krenn, A. Dereux, J. C. Weeber, E. Bourillot, Y. Lacroute, J. P. Goudonnet, G. Schider, W. Gotschy, and A. Leitner, "Squeezing the optical near-field zone by plasmon coupling of metallic nanoparticles," *Phys. Rev. Lett.* **82**, 2590-2593 (1999).
3. M. Quinten, A. Leitner, R. Krenn, and F. R. Aussenegg, "Electromagnetic energy transport via linear chains of silver nanoparticles," *Opt. Lett.* **23**, 1331-1333 (1998).
4. S. A. Maier, P. G. Kik, and H. A. Atwater, "Observation of coupled plasmon-polariton modes in Au nanoparticle chain waveguides of different lengths: Estimation of waveguide loss," *Appl. Phys. Lett.* **81**, 1714-1716 (2002).
5. S. A. Maier, P. E. Barclay, T. J. Johnson, M. D. Friedman, and O. Painter, "Low-loss fiber accessible plasmon waveguide for planar energy guiding and sensing," *Appl. Phys. Lett.* **84**, 3990-3992 (2004).
6. S. A. Maier and H. A. Atwater, "Plasmonics: localization and guiding of electromagnetic energy in metal/dielectric structures," *J. Appl. Phys.* **98**, 11101-11101 (2005).
7. I. A. Larkin, M. I. Stockman, M. Achermann, and V. I. Klimov, "Dipolar emitters at nanoscale proximity of metal surfaces: Giant enhancement of relaxation in microscopic theory," *Phys. Rev. B* **69**, 121403 (2004).
8. C. R. Simovski and A. J. V. S. A. Tretyakov, "Resonator mode in chains of silver spheres and its possible application," *Phys. Rev. E* **72**, 066606 (2005).

9. W. H. Weber and G. W. Ford, "Propagation of optical excitations by dipolar interactions in metal nanoparticle chains," *Phys. Rev. B* **70**, 125429-125421 (2004).
10. R. A. Shore and A. D. Yaghjian, "Travelling electromagnetic waves on linear periodic arrays of lossless spheres," *Electron. Lett.* **41**, (2005).
11. M. L. Brongersma, J. W. Hartman, and H. A. Atwater, "Electromagnetic energy transfer and switching in nanoparticle chain arrays below the diffraction limit," *Phys. Rev. B* **62**, 16356-16359 (2000).
12. V. A. Markel and A. K. Sarychev, "Propagation of surface plasmons in ordered and disordered chains of metal nanospheres," *Phys. Rev. B* **75**, 085426 (2007).
13. A. Alù and N. Engheta, "Theory of linear chains of metamaterial/plasmonic particles as subdiffraction optical nanotransmission lines," *Phys. Rev. B* **74**, 205436 (2006).
14. F. Falcone, T. Lopetegui, M. A. G. Laso, J. D. Baena, J. Bonache, M. Beruete, R. Marques, F. Martin, and M. Sorolla, "Babinet principle applied in the design of metasurfaces and metamaterials," *Phys. Rev. Lett.* **93**, 197401 (2004).
15. C. Girard and R. Quidant, "Near-field optical transmittance of metal particle chain waveguides," *Opt. Express* **12**, 6141-6146.
16. S. I. Bozhevolnyi, J. Erland, K. Leosson, P. M. W. Skovgaard, and J. M. Hvam, "Waveguiding in surface plasmon polariton band gap structures," *Phys. Rev. Lett.* **86**, 3008 (2001).
17. H. Ditlbacher, J. R. Krenn, G. Schider, A. Leitner, and F. R. Aussenegg, "Two-dimensional optics with surface plasmon polaritons," *Appl. Phys. Lett.* **81**, 1762-1764 (2002).
18. Z. W. Liu, J. M. Steele, W. Srituravanich, Y. Pikus, C. Sun, and X. Zhang, "Focusing surface plasmons with a plasmonic lens," *Nano Lett.* **5**, 1726-1729 (2005).
19. H. L. Offerhaus, B. E. van den Bergen, M., F. B. Segerink, J. P. Korterik, and N. F. van Hulst, "Creating Focused Plasmons by Noncollinear Phasematching on Functional Gratings," *Nano Lett.* **5**, 2144-2148 (2005).
20. J. M. Steele, Z. Liu, Y. Wang, and X. Zhang, "Resonant and non-resonant generation and focusing of surface plasmons with circular gratings," *Opt. Express* **14**, 5664-5670 (2006).
21. H. F. Ghaemi, T. Thio, D. E. Grupp, T. W. Ebbesen, and H. J. Lezec, "Surface plasmons enhance optical transmission through subwavelength holes," *Phys. Rev. B* **58**, 6779-6782 (1998).
22. L. Martín-Moreno, F. J. García-Vidal, H. J. Lezec, K.M.Pellerin, T. Thio, J. B. Pendry, and T. W. Ebbesen, "Theory of extraordinary optical transmission through subwavelength hole array," *Phys. Rev. Lett.* **86**, 1114-1117 (2001).
23. V. Lomakin, "Enhanced transmission through metallic plates perforated by arrays of subwavelength holes and sandwiched in between dielectric slabs," *Phys. Rev. B* **71**, 235117(235111-235110) (2005).
24. V. Lomakin, N. W. Chen, S. Q. Li, and E. Michielssen, "Enhanced transmission through two-period arrays of sub-wavelength holes," *IEEE Microwave Wirel. Comp. Lett.* **14**, 355-357 (2004).
25. R. E. Collin and F. J. Zucker, *Antenna theory, Part Two* (McGraw-Hill, New York, 1969).
26. G. Dolling, C. Enkrich, M. Wegener, C. M. Soukoulis, and S. Linden, "Simultaneous negative phase and group velocity of light in a metamaterial," *Science* **312**, 892-894 (2006).
27. A. Taflove, *Computational Electrodynamics: The Finite-Difference Time-Domain Method* (Artech House, Boston, MA, 1995).
28. L. B. Felsen and N. Marcuvitz, *Radiation and Scattering of Waves* (IEEE Press, Piscataway NJ, 1994).
29. A. Alù and N. Engheta, "On Role of Random Disorders and Imperfections on Performance of Metamaterials," presented at the 2007 IEEE Antennas and Propagation Society International Symposium, Honolulu, Hawaii, 2007.

1. Introduction

Free-standing metal nano-particles and chains thereof support many fascinating optical phenomena. Isolated metal nano-particles admit resonances for wavelengths up to an order of magnitude larger than their size [1]. These resonances are mediated by the metals' free-electrons at visible/near-infrared frequencies and permit the miniaturized implementation of various optical functionalities. Dense chains, viz. closely spaced linear arrays, of metal nano-particles support traveling waves (TWs) that propagate without radiation loss along, and are confined to a region near, the chain [2-15]. These TWs involve strong interactions between the chains' nano-particle constituents mediated by their individual resonances, which may depend on the particle shape and size [2-15]. They can have low group velocities, propagate in channels of deep subwavelength transverse dimensions, and efficiently traverse sharp chain bends [2, 4, 8-10, 15].

Metal nano-particle chains residing near metal surfaces can support an even richer variety of optical phenomena than free-standing ones. Indeed, when a metal nano-particle chain resides near a metal surface, the latter affects the propagation of TWs on the nano-particle chain. Likewise, the nano-particle chain interacts with surface plasmon polaritons (SPPs) traveling along the metal to air interface; SPPs are waves on flat metal surfaces with

transverse wavenumbers larger than the free-space wavenumber and hence confined to the interface. A thorough understanding of TWs supported by, and SPP scattering from, nano-particle chains residing near metal surfaces could enable the design of new subwavelength optical devices, including compactly integrated waveguides, resonators, and lasers, and spur the development of optical metamaterials. Unfortunately, extensive research into the optical properties of free-standing nano-particle chains and structured metal surfaces^{2, 4, 8-10, 16-24} notwithstanding, the study of optical TW guidance and SPP scattering by nano-particle chains residing near metal-dielectric surfaces has received only scant attention.

This paper investigates phenomena of optical guidance and scattering properties of nano-particle chains residing *on* a metal surface. Ordered and disordered, straight and sharply bent chains of gold parallelepiped shaped nano-particle residing directly on a gold surface, henceforth referred to as nano-bumps, are considered. By investigating frequency-wavenumber spectra of transient fields on chains generated in response to a localized excitation, source-excited as well as source free-fields supported by these structures are characterized. It is shown that nano-bump chains support TWs that are well confined to a region near the chain and have propagation lengths larger than those of TWs supported by free-standing chains comprising identical elements. The TWs are shown to be slow waves with respect to both space and SPP fields, and to be supported efficiently not only by straight ordered nano-bump chains but also by disordered chains and chains with sharp bends.

The outline of this paper is as follows. Section 2 elucidates the phenomenology of TW propagation on nano-bump chains to facilitate understanding the techniques and phenomena presented in subsequent sections. Section 3 describes implemented techniques for characterizing these waves. Sections 4 and 5 apply these techniques to the analysis of ideal and perturbed nano-bump chains, respectively. Section 5 presents this study's conclusions.

2. Definitions and phenomenology

Consider a periodic, infinite, and straight chain of metal nano-bumps residing on an interface between air and metal half-spaces (Fig. 1). The chain extends along and symmetrically straddles the x -axis; the chain's periodicity is $\Lambda \ll \lambda = 2\pi c/\omega$; here λ is the free-space wavelength, c is the free-space speed of light, and ω is the angular frequency. The metal interface coincides with the x - y plane; bumps aside, the space $z > 0$ is air-filled.

For specific bump geometries, periodicities, and frequencies, the chain supports TWs, viz. source-free fields that propagate along, and are confined to a region near, the chain. For $z > 0$, the electric field of the lowest order TW can be expressed as

$$\mathbf{E}_{\text{TW}}(\omega, \mathbf{r}) = \Psi(\rho_{yz}, \varphi_{yz}) \exp\left(-\left(k_{\text{TW}}^2 - (\omega/c)^2\right)^{1/2} \rho_{yz}\right) \exp(\pm i k_{\text{TW}} x), \quad (1)$$

where $\Psi(\rho_{yz}, \varphi_{yz})$ describes the field distribution in terms of transverse-to- x cylindrical coordinates $\rho_{yz} = (y^2 + z^2)^{1/2}$ and $\varphi_{yz} = \tan^{-1} z/y$ and $k_{\text{TW}}(\omega)$ is the (frequency-dependent) TW wavenumber. The field representation (1) indicates that the field propagates along the structure with the wavenumber k_{TW} and decays out of the chain in the ρ_{yz} dimension with a wavenumber k_ρ obtained via the relation $k_\rho^2 + k_{\text{TW}}^2 = (\omega/c)^2$.

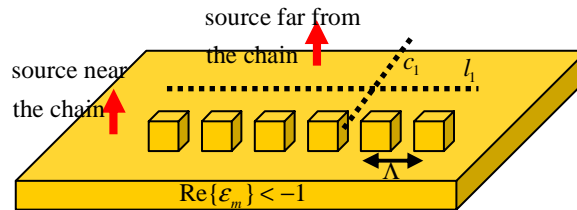


Fig. 1. Nano-chains on a metal surface. The line l_1 represents the field along the chain, and the line c_1 represent the field in the chain's cross-section.

The real part of the TW wavenumber $\text{Re}\{k_{\text{TW}}\}$ determines the TW phase velocity as well as the TW loss and confinement near the chain. The TW loss can be associated with dissipation

and radiation. The dissipation loss is always present due to the lossy nature of the metals in the optical regime. Two kinds of radiation loss can exist for the considered structure: Radiation loss into space waves out of the interface and radiation loss into SPPs along the interface; the first type of loss also may occur for free-standing chains but the second cannot. For TWs supported by a nano-bump chain to propagate without radiation loss, $\text{Re}\{k_{\text{TW}}(\omega)\}$ should be greater than both the free-space wavenumber $k_0 = \omega/c = 2\pi/\lambda$ and the real part of the (frequency-dependent) SPP wavenumber $k_{\text{spp}}(\omega)$, i.e. $k_0 < \text{Re}\{k_{\text{spp}}\} < \text{Re}\{k_{\text{TW}}\}$; when this condition is met, the TWs are slow waves with respect to both space waves and SPPs and they decay exponentially away from the chain; larger $\text{Re}\{k_{\text{TW}}\}$ imply stronger confinement. When $\text{Re}\{k_{\text{TW}}\} < k_0$, the TWs are fast (or leaky) waves with respect to both space and SPP fields. When $k_0 < \text{Re}\{k_{\text{TW}}\} < \text{Re}\{k_{\text{spp}}\}$, the TWs are fast (or leaky) with respect to the SPPs but slow with respect to space waves. In this paper we focus on the case $\text{Re}\{k_{\text{spp}}\} < \text{Re}\{k_{\text{TW}}\}$ where no radiation losses occur. An investigation of the fast wave regime will be presented elsewhere.

The imaginary part $\text{Im}\{k_{\text{TW}}\}$ determines the propagation length of the TW, which, in the regime investigated here, is finite due to dissipation. The dispersion relation also determines the TW's group velocity: flat regions in the dispersion curve imply low group velocity, meaning that pulsed TWs can be delayed compared to free-space fields or SPPs.

The resonances supported by individual nano-bumps play an important role in the chain's waveguiding properties [2, 4, 8-10, 13]. Individual nano-bumps support resonances, viz. source-free electromagnetic fields confined to the region near the bump and oscillating at complex resonance frequencies ω_p (with corresponding resonance wavelengths $\lambda_p = 2\pi c/\omega_p$) determined by the nano-bump's dimensions as well as the nano-bump's and metal surface's constitutive parameters. In the mid-infrared regime, where many metals are nearly perfect conductors, bumps that are much taller than wide act as monopoles with resonant wavelengths $\lambda_p \approx 4(\text{bump height})/q$, $q = 1, 2, \dots$. For frequencies approaching the metal plasma frequency, e.g. in the near-infrared or visible regimes, and depending on the nano-bump shape, resonances can be supported by nano-bumps of deep subwavelength size. Due to the presence of the metal surface, the resonant frequencies of the nano-bumps are substantially lower than the resonant frequencies of free-standing nano-particles of the same shape and size. This, in turn, implies that the TW properties of nano-bump chains are quite different from those of free-standing chains. When a nano-bump is excited by an external field, the bump's resonance frequencies/wavelengths appear as complex poles in the frequency dependence of the nano-bump's response to the excitation. Therefore, as the wavelength λ is scanned through $\lambda_r = \text{Re}\{\lambda_p\}$, the magnitude of the field response exhibits strong peaks and its phase exhibits rapid variations.

For a TW to exist, the fields scattered from the nano-bumps should constructively interfere along the chain and destructively out of the chain. From the theory of TW antennas²⁵, such condition is obtained for wavelengths greater than the resonant wavelength of the isolated nano-bumps (assuming that the wavelength of operation is near a single resonance wavelength). The TWs supported behave quite differently when the individual nano-bumps are near- or non-resonant. Indeed, resonances lead to strong interactions between the nano-bumps along the chain, which, in turn, leads to large TW wavenumbers and strong TW confinement near the chain [2, 4, 8-10, 13]. These strongly confined fields can be excited efficiently by an impressed (e.g. localized) source since their modal field distribution overlaps significantly with the source's near-fields. Due to their strong confinement, these TWs can be transmitted efficiently through chains with sharp bends. On the other hand, due to the resonant dissipation in the chain elements, these TWs may have a small propagation lengths (i.e. strong decay). In addition, these TWs can be significantly affected by chain irregularities (e.g., disturbances in chain element locations and sizes). Away from resonances, interactions between chain elements are weak. The corresponding TWs are characterized by wavenumbers that approach the SPP or free-space wavenumber. As a result, the TWs are less confined to the region near the chain. In the case of chains with sharp bends, this reduced confinement leads to reduced transmission through the bend. On the other hand, the weakly confined TWs are

expected to lead to a large propagation length because the dissipation in the chain elements is weak. In addition, due to a weak confinement, irregularities in the chain element properties are expected to only mildly affect the TWs.

Finally, it is noted that the propagation length of TWs supported by the nano-bump chains may be larger than those of free-standing chains comprising identical nano-particles for the same confinement to the region near the chain (i.e. the same cross-sectional decay rate). The reason for the increase of the TW propagation length is the increase of the resonant wavelength further from the metal plasma frequency.

Sections 4 and 5 elucidate the above phenomenology for ideal and perturbed nano-bump chains, respectively. Characterization techniques used in the study of these structures are discussed next.

3. Characterization techniques

To study the TW phenomena discussed in Section 2, we considered nano-bump chains comprising gold bumps of square cross-section $w \times w$ and height h residing on a gold interface. Gold's constitutive parameters are described by a Drude model with plasma frequency $\omega_{\text{plasma}} = 1.32 \times 10^4 \text{ THz}$ and damping parameter $\Gamma = 1.2 \times 10^3 \text{ THz}$ [26]. To model a wide array of phenomena, the chains were excited by transient fields generated by a short electric dipole $\mathbf{J}(t, \mathbf{r}) = \hat{\mathbf{z}} e^{t^2/(2\tau^2)} \cos(\omega_0 t) \delta(\mathbf{r} - \mathbf{r}_0)$; here \mathbf{r}_0 is the dipole location, ω_0 the carrier frequency, and τ the pulse's temporal width; $1/\tau$ determines the pulse's bandwidth. This dipole models an excitation due to a pin-hole or a near-field probe (e.g. in an NSOM setup).

Upon interaction of this dipole's field with the nano-bump chain, three types of fields can be generated: space fields scattered out of the metal surface, SPPs propagating along the surface, and TWs tracking the chain. Space fields can be excited by the dipole irrespective of its position; once excited they dominate the field far from the surface. SPPs can be efficiently excited by a dipole placed near the metal surface; once excited and away from the chain they typically dominate the total field near the surface for distances from the source on the order of the SPP propagation length or less; these SPPs can be scattered/reflected/diffracted by the nano-bump chain. TWs supported by the nano-bump chain can be excited efficiently by localized sources placed near the chain; once excited they typically dominate the total field along the chain for distances from the source of the order of the TW propagation length or less.

Knowledge of fields along a chain provides important information about the TWs supported by the chain. Consider a transient field $\mathbf{E}(t, x)$ observed (for fixed and sufficiently small y and z) near an *infinite* nano-bump chain. Assume the field is excited by a broadband dipole placed near the chain. Define the space-time Fourier transform of the field $\mathbf{E}(t, x)$ as

$$\hat{\mathbf{E}}(\omega, k_x) = \int_{-\infty}^{\infty} dt \int_{-\infty}^{\infty} dx \mathbf{E}(t, x) e^{i(\omega t - k_x x)}. \quad (2)$$

Assuming that the field is dominated by the TWs and using Eq. (1), $\hat{\mathbf{E}}(\omega, k_x)$ can be approximated as

$$\hat{\mathbf{E}}(\omega, k_x) \approx \hat{\mathbf{E}}_{\text{cs}} \left(\frac{a_1}{k_x - k_{\text{TW}}(\omega)} + \frac{a_2}{k_x + k_{\text{TW}}(\omega)} \right) \quad (3)$$

where $\hat{\mathbf{E}}_{\text{cs}}(\omega, k_x) = \Psi(\rho_{yz}, \varphi_{yz}) \exp(-(k_{\text{TW}}^2 - (\omega/c)^2)^{1/2} \rho_{yz})$ is the TW cross-sectional field distribution and $a_{1,2}$ are the amplitudes of the TWs propagating to the right and left of the source. The TW wavenumbers $\pm k_{\text{TW}}$ appear as poles in the spectral field $\hat{\mathbf{E}}(\omega, k_x)$. It follows that for every ω , the k_x -dependence of the spectral field $\hat{\mathbf{E}}(\omega, k_x)$ exhibits peaks. The peak maxima $(\omega, k_x \approx \pm \text{Re}\{k_{\text{TW}}(\omega)\})$ in the (ω, k_x) plane are indicative of $\text{Re}\{k_{\text{TW}}(\omega)\}$; the peak widths approximate the dependence $\text{Im}\{k_{\text{TW}}(\omega)\}$.

In practice, we analyzed fields near *finite* chains using a finite difference time domain solver [27] that incorporates impedance boundary conditions to account for the presence of the metal surfaces [28] thus avoiding the computationally expensive discretization of metal volumes. The upper half-space was discretized with cell size chosen in the range $\Delta x = \Delta y = \{12.5 \text{ nm} - 25 \text{ nm}\}$ and $\Delta z = \{5 \text{ nm} - 10 \text{ nm}\}$ with time discretization of $\Delta t = 0.8 \Delta x / c$. The computational domain was terminated with perfectly matched layers [27].

Consider a finite chain comprising of nano-bumps on total length $D \gg \lambda$ that, as before, is excited by a dipole residing near the chain. The chain's edges affect the TW field distribution along the chain in two ways. First, TWs reflected from the chain edges appear and the left and rightward TWs combine into a standing wave. Second, near the chain ends the field complicated structure and changes rapidly because of edge scattering and the generation of higher-order modes. To eliminate the latter effect, a weighted Fourier transform is introduced via

$$\hat{\mathbf{E}}_D(\omega, k_x) = \int_{-\infty}^{\infty} \int_{-\infty}^{\infty} w(x) \mathbf{E}(t, x) e^{i(\omega t - k_x x)} dt dx, \quad (4)$$

where $w(x)$ is a window function that is flat in the center section of the nano-bump chain and gradually approaches zero near its ends. When $\text{Im}\{k_{\text{TW}}\} \gg D$, i.e. when the TW propagation distance is smaller than the chain length, and the source is located far from both chain edges, the chain edges do not have a significant effect and $\hat{\mathbf{E}}_D(\omega, k_x) \approx \hat{\mathbf{E}}(\omega, k_x)$. In this case, both dependencies $\text{Re}\{k_{\text{TW}}(\omega)\}$ and $\text{Im}\{k_{\text{TW}}(\omega)\}$ can be found from the transient field $\mathbf{E}(t, x)$ by studying $\hat{\mathbf{E}}_D(\omega, k_x)$ in (4). When $\text{Im}\{k_{\text{TW}}\} < D$, i.e. when the TWs propagate without noticeable decay over the length of the chain, then $\hat{\mathbf{E}}_D(\omega, k_x) \approx \tilde{a}_1 \hat{w}(k_x - k_{\text{TW}}(\omega)) + \tilde{a}_2 \hat{w}(k_x + k_{\text{TW}}(\omega))$, where \tilde{a}_1 and \tilde{a}_2 are standing wave amplitudes that characterize both the strength of the excitations of the leftward and rightward propagating TWs as well as their reflections from the two chain edges. In this case, one cannot easily find the dependence $\text{Im}\{k_{\text{TW}}(\omega)\}$ from $\mathbf{E}(t, x)$ and $\hat{\mathbf{E}}_D(\omega, k_x)$. However, since $D \gg \lambda$, the locations of the maxima of $\hat{\mathbf{E}}_D(\omega, k_x)$ in the (ω, k_x) plane still approximate well the dependence $\text{Re}\{k_{\text{TW}}(\omega)\}$. In addition, one can find the standing wave amplitudes \tilde{a}_1 and \tilde{a}_2 .

It is noted that there exist other approaches to calculate dispersion relations of infinitely periodic chains of particles [27]; one is to model only a single cell of the chain and assume periodic boundary conditions. An advantage of the procedure outlined above is that it allows characterizing dispersion properties not only of infinite periodic chains but also of finite chains with periodically or randomly distributed chain elements. In addition, it directly provides information about the strength of the TW excitation for a particular frequency/wavelength and TW wavenumber. It also can provide information about the reflection properties of truncated chains.

4. Traveling waves on straight ordered nano-bump chains

As a precursor to studying fields on nano-bump chains, this section first characterizes phenomena of scattering by isolated bumps. To this end, consider nano-bumps of width $w = 100 \text{ nm}$ and height $h = 70 \text{ nm}, 100 \text{ nm},$ and 150 nm (see insert to Fig. 2); the center of the nano-bumps' bottom facets coincides with the origin. These nano-bumps were excited by an SPP which, in turn, was excited by a transient dipole with $\omega_0 = 1.88 \times 10^{15} \text{ rad/s}$ and $\tau = 5.08 \times 10^{-14} \text{ s}$ residing at $\mathbf{r}_0 = (-8 \mu\text{m}, 50 \text{ nm}, 50 \text{ nm})$, i.e., far from the nano-bump. The scattered field was obtained by computing fields in the presence and absence of the nano-bump and subtracting the latter from the former. The spectral content of the scattered field (normalized with respect to the magnitude of the Fourier transform of $\mathbf{J}(t, \mathbf{r})$) at $\mathbf{r} = (100 \text{ nm}, 50 \text{ nm}, 100 \text{ nm})$ near the nano-bump is shown in Fig. 2. The scattered field exhibits the resonant behavior as manifested by peak maxima at $\lambda = 0.568 \mu\text{m}, 0.755 \mu\text{m}$ and $1.05 \mu\text{m}$ for $h = 70 \text{ nm}, 100 \text{ nm},$ and 150 nm , respectively. The peak maxima approximate the resonance wavelengths λ_r . Note that these resonance wavelengths significantly exceed the

size of the nano-bumps. As shown below, the wave guiding properties of nano-bump chains significantly depend on the difference between the wavelength of operation and the resonance wavelength of the isolated nano-bumps comprising the chain. Also note that for the chosen structure and excitation parameters the size of the nano-bumps is greater than the skindepth in gold. As a result, the resonance frequencies/wavelengths depend both on the nano-bumps' shape and size. This is in contrast to the often considered static/quasi-static regime, where the resonant frequencies depend only on the chain elements' shape [2-13].

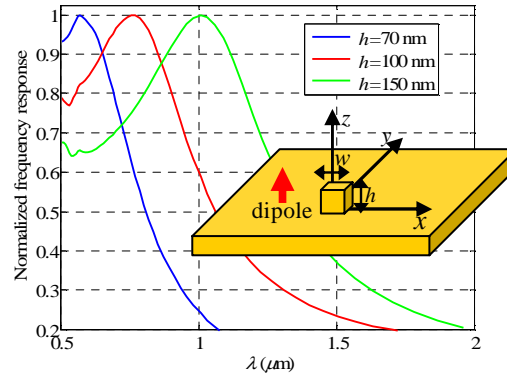


Fig. 2. Electric field normalized frequency response of isolated metal nano-bumps as shown in the insert. The vertical axis is defined as normalized to the maximum magnitude of the time Fourier transforms of the electric field at $\mathbf{r} = (100 \text{ nm}, 50 \text{ nm}, 100 \text{ nm})$ and exciting current at $\mathbf{r}_0 = (-8 \mu\text{m}, 50 \text{ nm}, 50 \text{ nm})$. The nano-bumps have a square cross-section of size $w \times w$ with $w = 100 \text{ nm}$ in the $x-y$ plane and three heights h . The normalized frequency response is defined as the normalized to the maximal value magnitude of the ratio between the time Fourier transforms of the electric field and exciting current.

We also studied resonant properties of free-standing nano-parallelepipeds of the dimensions identical to those of the nano-bumps. It was found that the corresponding resonant wavelengths were noticeably smaller than those of the nano-bumps. For example, the resonant wavelengths for the nano-parallelepipeds of heights $h = 70 \text{ nm}$, $h = 100 \text{ nm}$, and 150 nm were obtained at $\lambda = 0.441 \mu\text{m}$, $\lambda = 0.476 \mu\text{m}$, and $\lambda = 0.517 \mu\text{m}$, respectively (for the cross-sectional size of $w = 100 \text{ nm}$).

To characterize wave phenomena supported by straight periodic nano-bump chains, consider a chain of $N = 160$ bumps of width and height $w = h = 100 \text{ nm}$, and periodicity $\Lambda = 200 \text{ nm}$; the chain length $D = 32 \mu\text{m}$ (Fig. 1). The chain symmetrically straddles the $+x$ -axis; the center of the bottom facet of the first (leftmost) bump coincides with the origin.

Figure/snapshot/movie 3 shows the temporal evolution of the electric field $|\mathbf{E}(t, x)|$ observed in the horizontal plane $z = 3h/2$, i.e. 50 nm above the nano-bump's top face, excited by the above dipole moved to $\mathbf{r}_0 = (16 \mu\text{m}, 10 \mu\text{m}, 150 \text{ nm})$. The dipole is located sufficiently far from the chain so that the chain, for all practical purposes, is excited by an SPP. It is evident that the chain reflects part of the SPP, while the chain's TWs are only weakly excited from the chain edges.

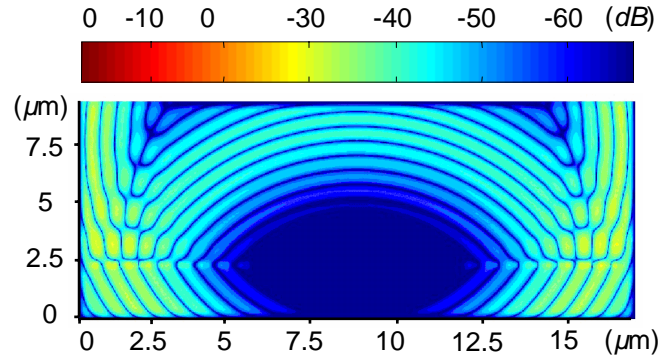


Fig. 3. Time evolution of the electric field supported by a straight chain of nano-bumps in Fig. 1(b). The chain comprises $N = 160$ of gold nano-bumps of width and height $w = h = 100$ nm with periodicity $\Lambda = 200$ nm. The excitation dipole resides at $(16\mu\text{m}, 10\mu\text{m}, 150\text{nm})$, i.e. it is far from the chain. The field is computed at the plane $z = 150$ nm.

The strength of the TW excitation can be increased significantly by allowing the dipole to reside near the chain, thereby generating a near-field with components matching the TW field distribution $\Psi(\rho_{yz}, \varphi_{yz})$ and wavenumber k_{TW} . Figure/snapshot/movie 4 shows the temporal evolution of $|\mathbf{E}(t, x)|$ in the $z = 3h/2$ plane when the dipole resides as $\mathbf{r}_0 = (-200\text{nm}, 0, 150\text{nm})$, that is near the left edge of the chain. Two waves are observed. The wave with a greater velocity corresponds to the SPP supported by the metal surface, whereas the wave with a lower velocity is the TW supported by the chain. The TW exhibits dispersion, i.e. the pulsed field changes spatial width while propagating. In addition, the field has a stronger confinement in the left part of the TW spatial extension, which is due to the fact that slower wave components have a larger propagation wavenumber. The visual reduction of the confinement in the front part of the chain spatial extension is attributed to the reduced excitation of the faster field components. The observed field behavior is characterized in the following results and discussions.

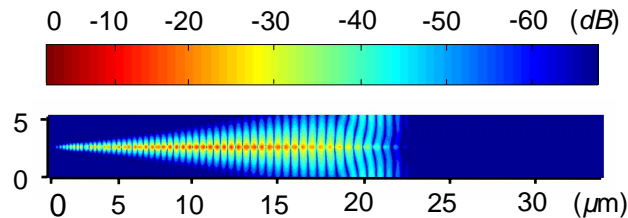


Fig. 4. Time evolution of the electric field supported by a straight nano-bump chain. The chain's parameters are as in Fig. 3 (i.e. $N = 160$, $w = h = 100$ nm, and $\Lambda = 200$ nm). The excitation dipole resides at $(-200\text{nm}, 0, 150\text{nm})$, i.e. near the left edge of the chain. The field is computed at the plane $z = 150$ nm.

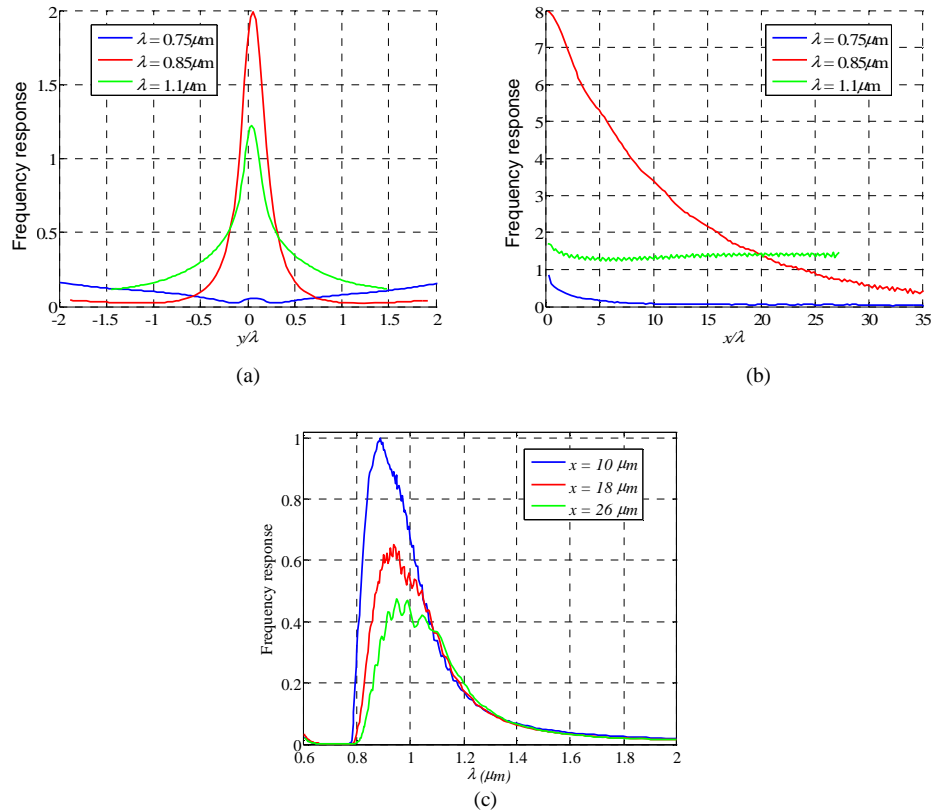


Fig. 5. Wave guiding characteristics of a straight nano-nano-bump chain with parameters in Fig. 3 (i.e., $N=160$, $w=h=100$ nm, and $\Lambda=200$ nm) excited by a dipole at $(-200\text{nm}, 0, 150\text{ nm})$. (a) Electric field frequency response in the transversal chain cross-section along the line c_1 in Fig. 1 that resides at $x=16 \mu\text{m}$, $z=150$ nm; (b) Electric field frequency response along the line l_1 in Fig. 1 that resides at $y=0$, $z=150$ nm; (c) Electric field frequency response at the points $(10 \mu\text{m}, 0, 2h)$, $(18 \mu\text{m}, 0, 2h)$, and $(26 \mu\text{m}, 0, 2h)$ on the line l_1 . The frequency response is defined as the magnitude of the ratio between the time Fourier transforms of the electric field and exciting current.

To quantify the wave guiding properties of the chain of nano-bumps, Figs. 5(a) and 5(b) show the (normalized) spectral content of the field recorded along a line the chain cross-section on the line c_1 at $x=16 \mu\text{m}$, $z=150$ nm, and along the chain on the line l_1 at $y=0$, $z=150$ nm, respectively (Fig. 1). The window function in (4) was chosen as $w(x) = \{\text{erfc}[40(x-0.9D)/D] + \text{erfc}[40(0.1D-x)/D]\}/4$, where $\text{erfc}(x)$ is the complementary error function. For $\lambda < 0.755 \mu\text{m}$, i.e. for wavelengths smaller than the resonance wavelength of the isolated nano-bump λ_r (of height $h=100$ nm), neither propagation nor field confinement is observed. For $\lambda = 0.85 \mu\text{m}$, i.e., slightly larger than λ_r , a TW is excited efficiently. The TW field is strongly confined near the chain [Fig. 5(a)] but at the same time it is strongly attenuated while propagating along the chain [Fig. 5(b)]. The strong attenuation is due to the strong dissipation in the metal associated with resonant fields in the chain elements and with strong fields confined to the bumps and metal surface. For $\lambda = 1.1 \mu\text{m}$, i.e., for a wavelength significantly larger than the isolated nano-bump's resonance wavelength, the TW propagates along the chain with a weak attenuation. However, the TW excitation strength is relatively weak and the TW is not well confined near the chain. The decrease of the excitation strength, lack of confinement, and weak attenuation are due to the fact that far from resonance the nano-bumps are weak scatterers. Note that for $\lambda = 1.1 \mu\text{m}$, i.e., when the TW propagation length is large, the field does not decay monotonously along

the chain (Fig. 5(b) but rather has a minimum (at $x/\lambda \approx 7$). In addition, there are some ripples in the field dependence. This behavior is obtained because the TW propagation length is significantly larger than the length of the chain. As a result the TW is scattered from the chain ends thus leading to the existence of a standing type TW. Figure 5(c) shows the wavelength dependence of the (normalized) spectral content of the field recorded at three points on the line l_1 (Fig. 1). In agreement with Figs. 5(a) and 5(b), no propagation occur for $\lambda < \lambda_r$. For wavelengths only slightly above λ_r , the TW magnitude is very weak. The TW transmission peak is obtained around $\lambda = 0.95 \mu\text{m}$. For $\lambda > 0.95 \mu\text{m}$, the TW magnitude decreases. The decrease of the TW magnitude for $\lambda_r < \lambda < 0.95 \mu\text{m}$ is due to an increase of the loss associated with the proximity of the resonance of the individual nano-bumps. The decrease of the TW field for $\lambda > 0.95 \mu\text{m}$ is due to a decrease of the TW excitation strength associated with weaker TW confinement.

Figure 6 shows the field $\hat{\mathbf{E}}_D$ defined in Eq. (4) as a function of normalized λ (or ω) and k_x . To evaluate the temporal Fourier transform, the time domain response was computed and recorded at the required locations for times long enough so that all resonant fields decayed to a relative value of about 10^{-8} . The obtained dispersion curve is located below the dispersion curve of the SPP supported by the metal surface (blue line in Fig. 6) so that the TW is a slow wave with respect to both free-space and SPP fields. In the first Brillouin zone for $k_x \Lambda < \pi$, the maximum value of the normalized wavenumber $k_x/k_0 \approx 2$ for $\lambda \approx 0.77 \mu\text{m} \approx \lambda_r$. For this value of k_x/k_0 , the field is strongly confined near the chain as shown in Fig. 5(a). It was found that k_x/k_0 can be larger for smaller periodicities Λ . In addition, it is evident that the maxima of the dispersion curve are well-pronounced in the range $0.4 < k_x \Lambda/\pi < 0.7$ and less pronounced otherwise. The decrease of the maxima strength for $k_x \Lambda/\pi < 0.4$ is due to the decrease of the TW excitation for this range of relatively weak TW confinement near the chain. For $k_x \Lambda/\pi > 0.7$, the decrease of the magnitude is due to the increased TW decay along the chain caused by resonant dissipation. It should be noted that, unlike the dispersion curves of free-standing chains of nano-spheres of sub-skindepth size [2, 4, 8-10], the dispersion curve in Fig. 6 does not exhibit a low group velocity together with a non-vanishing phase velocity. This is associated with differences in the scattering properties of isolated nano-bumps and sub-skindepth nano-spheres. Some of our additional simulations indicate that bands of low group velocity with non-vanishing phase velocity can exist in the case of chains of nano-particles near metal or dielectric surfaces when proper conditions on the particle size/shape and particle-surface distance are satisfied. The study of this regime will be presented elsewhere.

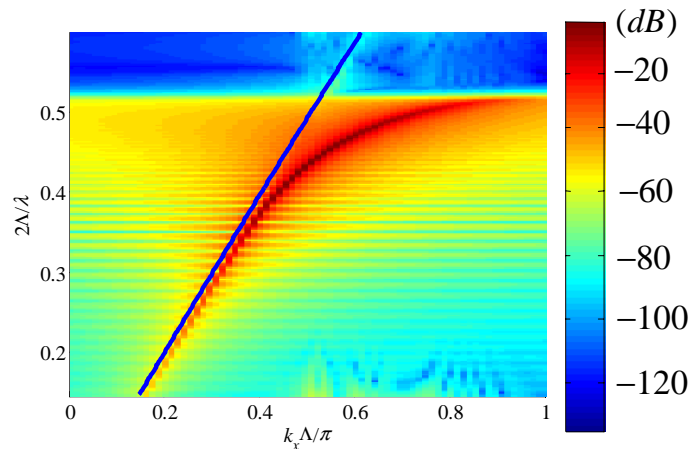


Fig. 6. Space-time Fourier transform $|\mathbf{E}_D|$ along the chain in Fig. 1(b) excited by a transient dipole with parameters in Fig. 2 residing at $(-200 \text{ nm}, 0, 150 \text{ nm})$. The chain parameters are as in Fig. 3 (i.e. $N=160$, $w=h=100 \text{ nm}$, and $\Lambda=200 \text{ nm}$). The blue line is the dispersion curve of the SPP supported by the metal surface.

The qualitative behavior of $\hat{\mathbf{E}}_D$ in Fig. 6 for nano-bumps of different heights (e.g. $h = 70\text{ nm}$ and 150 nm as in Fig. 2) share the same characteristics including the behavior of the maxima/dispersion curves. Quantitatively, however, the maxima/dispersion curves are shifted up and down for smaller ($h = 70\text{ nm}$) and larger ($h = 150\text{ nm}$) heights respectively.

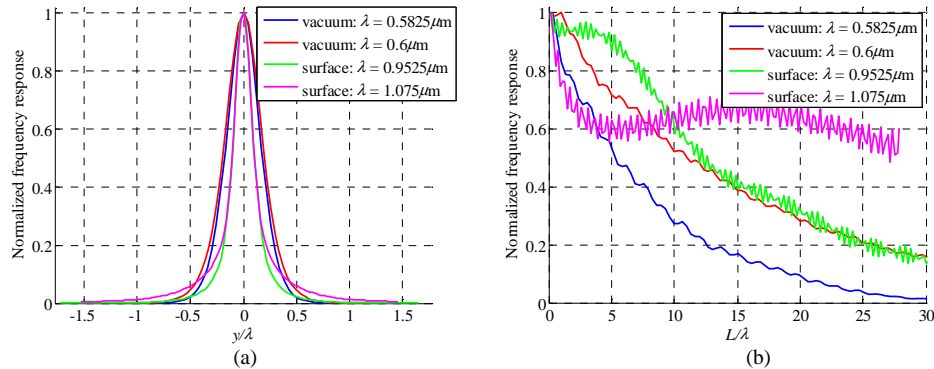


Fig. 7. Comparison between nano-bump chains and free-standing chains of nano-cubes. The two chain types have identical size, excited by an identical source, and the field is calculated along the same line as in Fig. 5. (a). Normalized frequency response in the transversal chain cross-section; (b). Frequency response along the chain. The wavelengths are chosen to render nearly identical cross-sectional decay rate [Fig. 7(a)]. The normalized frequency response is defined as normalized to the maximal value magnitude of the ratio between the time Fourier transforms of the electric field and exciting current.

To demonstrate effects introduced by the presence of a metal surface, Fig. 7 compares the propagation length of the TWs supported by the nano-bump chains in Fig. 5 and chains of free-standing gold nano-cubes of identical size. The excitation dipole and observation locations are identical to those in Fig. 5. For proper comparison between the two chains, the results are shown for the wavelengths chosen to render the cross-sectional decay rate (nearly) identical [Fig. 7(a)]. From Fig. 7(b), the propagation length of the nano-bump chain is significantly larger than that of the free-standing nano-cube chain. One of the reasons for the increase of the TW propagation length for the nano-bump chain is a higher separation between the metal plasma wavelength and resonant wavelength of isolated nano-bumps as compared to the resonant wavelength of free-standing nano-cubes. The observed increase of the propagation length is important in applications incorporating wave guiding structures. It is noted that the properties of the TWs supported by chains near a metal surface qualitatively remain unchanged in the case where the half-space above the surface is filled with a dielectric material. Further study is being pursued to characterize effects introduced by more complicated substrates comprising dielectric-metal layered composites.

5. Traveling waves on disordered and bent nano-bump chains

This section first studies the influence of disorder in the location and size of the nano-bumps on the nano-bump chain properties. Then, it describes properties nano-bump chains with sharp bends.

5.1 Straight disordered chains

Real-world nano-bump chains exhibit random variations in nano-bump sizes, shapes, and positions. To assess tolerances allowed for these parameters, two types of disordered linear chains of nano-bumps were investigated. In the first type, the nano-bumps were randomly displaced along the y direction in the range $\{-\chi_L w, \chi_L w\}$ with uniform distribution. In the second disordered chain type, the height or the width of the nano-bumps was varied randomly with uniform distribution in the range $\{h(1-\chi_h), h(1+\chi_L)\}$ or $\{w(1-\chi_w), w(1+\chi_w)\}$, respectively. All other parameters were as in Figs. 5 and 6.

Figure/snapshot/movie 8(a) and 8(b) show field time evolution along straight chains with disorder in the position and in the height, respectively, for $\chi_L = \chi_h = 0.25$. The format of the movies is as in Figs. 4. It is observed that for the chain with randomness in the nano-bump position a TW is still supported efficiently even for the chosen relatively large disorder. On the other hand, the TW decays much faster for the chain with randomness in the height. A behavior similar to that in Fig. 8(b) was obtained in the case of disorder in the nano-bump width; the corresponding results, therefore, are not shown.

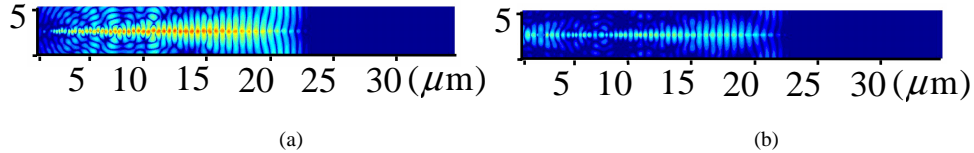


Fig. 8. Time evolution of the electric field supported by periodic chains of nano-bumps when the excitation dipole with parameters in Fig. 2 resides at $(-200\text{ nm}, 0, 150\text{ nm})$. The parameters of the nano-bumps are as in Fig. 3 and the scale is identical to that in Fig. 4. The field is computed at the plane $z = 150\text{ nm}$. (a) Disorder in displacement with $\chi_L = 0.25$ and (b) disorder in height with $\chi_h = 0.25$.

To characterize effects introduced by randomness on the TW propagation, Figs. 9(a), 9(b), and 9(c) show electric fields along the chains with disorder in position, height, and width, respectively, on the line l_1 for two values of the wavelength $\lambda = 0.85\ \mu\text{m}$ (near λ_r) and $\lambda = 1.1\ \mu\text{m}$ (far from λ_r) and two values of χ_L, χ_w, χ_h . The format of the figures is identical to that of Fig. 5(b). It is evident that the propagation length of the TW decreases in all cases [Fig. 9(a)-9(c)] with increase of χ_L, χ_h , and χ_w . It is also evident that the disorder has a much stronger effect in the case where λ is close to λ_r . It is remarkable, that for the chains with positional disorder [Fig. 9(a)] only for very large χ_L does one observe noticeable decrease of the TW propagation length. On the other hand, for the chain with disorder in the height and width [Figs. 9(b) and (c)], even weak disorders lead to significant decrease of the TW propagation length. In addition, TWs on these chains [Figs. 9(b) and (c)] are excited much weaker.

To further compare the dispersion relations of ordered and disordered chains, Fig. 10(a) and (b) show Fourier transformed field $\hat{\mathbf{E}}_D$ as a function of normalized λ (or ω) and k_x for the chains with randomness in the nano-bump position and height, respectively, with $\chi_L = \chi_h = 0.25$; the format of the figures is identical to that of Fig. 6. In Fig. 10(a), the dispersion relation of the chain is well pronounced. The dispersion curve is similar to that of the ordered chain in Fig. 6 with some distortion/widening near $k_x \Lambda = \pi$ and corresponding values of λ (or ω). On the other hand, in Fig. 10(b), the dispersion curve is significantly distorted thus indicating that for chains with disorder in the element size, the TWs are supported much less efficiently. It is also noted that the distortion of the dispersion curve is minor for longer wavelengths where k_{TW} is small and the TWs are not well confined to the region near the chain. On the other hand the distortion is well pronounced for shorter wavelength where k_{TW} is large and the TWs are well confined to the region near the chain. Chains with disorder in the nano-bump width exhibited a behavior similar to that in Fig. 10(b); the corresponding results, therefore, are not shown.

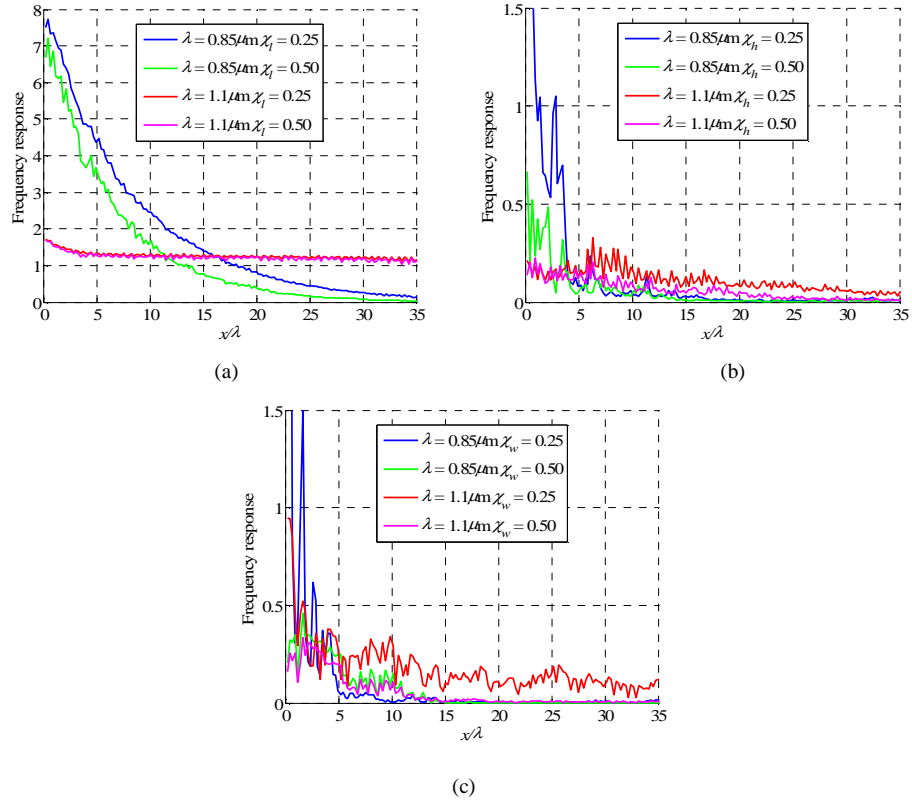


Fig. 9. Electric field normalized frequency response along the line l_1 in Figs. 1(b) and 5 for chains excited by a dipole with parameters in Fig. 2 residing at $(-200\text{nm}, 0, 150\text{nm})$ with disorder in (a) displacement, (b) height, and (c) width for different randomness parameters and wavelengths. The frequency response is defined as the magnitude of the ratio between the time Fourier transforms of the electric field and exciting current.

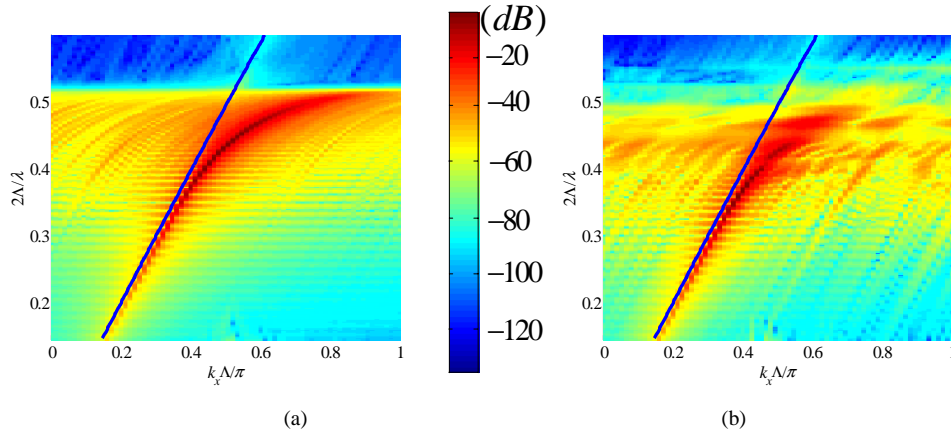


Fig. 10. Spectral field $|E_p|$ along the chain in Fig. 1(b) excited by the dipole with parameters in Fig. 2 residing at $(-200\text{nm}, 0, 150\text{nm})$. (a) disorder in displacement with $\chi_L = 0.25$ and (b) height $\chi_h = 0.25$.

The reason for the increased decay of TWs for chains with disorder in the nano-bump's height is that modifications in the nano-bump's height lead to a shift of the resonance

wavelength of the nano-bumps. The effect of the shifted resonance wavelength is much stronger than the effect of shifted nano-bump position. Indeed, the exact alignment of the nano-bumps is not very important for any type of positional disorder (e.g. for disorder in the separation between the chain elements) as long as it is within the range of the field confinement. On the other hand, the shift of the resonance wavelength reduces the interaction strengths between the nano-bumps and increases the loss due to the scattering from the disordered chain elements significantly. It should be noted the observed behavior also occurs in the case where the bump's size is randomly scaled without changing the bump's shape. This behavior is different than that obtained for chain elements comprising metal nanoparticles of sub-skindepth size [29]. This is because in the later case the resonances are nearly independent of the element size.

5.2 Ordered chains with sharp bends

The near-field nature of the interaction between the nano-bumps allows efficient TW propagation even through chains with sharp bends. To demonstrate such propagation phenomena, consider a chain of nano-bumps with a bend of 90° (Fig. 11). The chain consists of two identical sections, each having $N = 75$ nano-bumps arranged periodically. The chain parameters are identical to those chosen in Figs. 5-7.

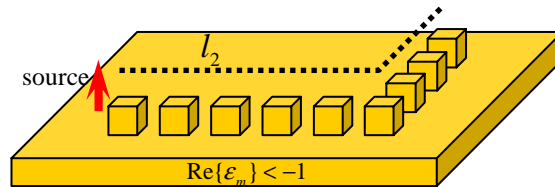


Fig. 11. Chain of nano-bumps with a 90° bend. The chain consists of two identical sections, each having $N = 75$ nano-bumps arranged periodically. The chain parameters are identical to those chosen in Figs. 5-7.

Figure/snapshot/movie 12(a) shows the time evolution of the electric field in the plane $z = 150$ nm. Two types of waves are observed. One is the SPP that propagates along the surface from the exciting dipole as a cylindrical wave and is reflected from the chain. The other wave type is a transient TW supported by the chain. It is evident that the TW has a velocity smaller than the velocity of the SPP and therefore it has a larger time delay. It is further observed that the TW is transmitted through the chain bend rather efficiently. Some field components that are reflected and scattered from the chain end are also present.

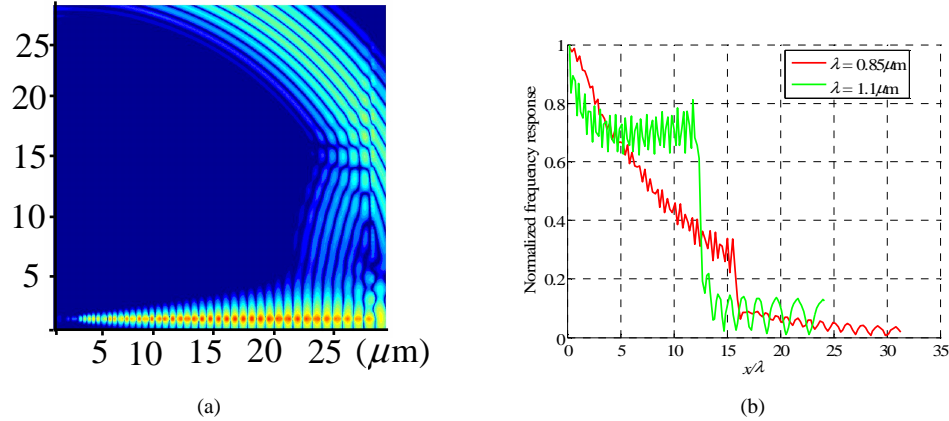


Fig. 12. (a). Time evolution of the electric field supported by the chain in Fig. 11 for the field computed on the plane $z=150\text{ nm}$ (the scale is identical to that in Fig. 4.); (b) Electric field frequency response along the line l_2 in Fig. 11. The normalized frequency response is defined as normalized to the maximal value magnitude of the ratio between the time Fourier transforms of the electric field and exciting current.

To further characterize the field transmission through the bend, Fig. 12(b) shows the electric field along the chain for three frequencies as in Fig. 5(b). It is observed that for $\lambda=0.85\ \mu\text{m}$, i.e. for the wavelength just above the resonance wavelength in Fig. 2, the transmission through the bend is very strong with the ratio of the field before and after the bend of 0.35 (however, as in Fig. 5, the decay rate of the TW is relatively high). The significant transmission is due to the strong confinement within the chain, which leads to primarily near field nature of the interaction between the nano-bumps in the chain. For $\lambda=1.1\ \mu\text{m}$, i.e. for the wavelength significantly above the resonance wavelength, the transmission through the bend is relatively weak with the ratio between the fields from the two sides of the bend of 0.14 (however, the decay rate is low). The weak transmission is due to reduced confinement of the TW field near the chain. It should be noted that the transmission can be further increased by incorporating special chain elements or modifying the nano-bump arranging near the bend, e.g. making it slightly smoother.

6. Summary

Optical wave phenomena supported by ordered and disordered chains of metal nano-bumps were investigated numerically and analytically. Special attention was paid to phenomena of TW guidance along the chains. The analysis was performed by finding the fields supported by the chains that were excited by a transient localized source and then studying the frequency-wavenumber spectra of these fields. Such analysis allowed characterizing source-excited as well as source-free fields including assessments of the TW excitation strength.

Isolated nano-bumps support resonances for wavelengths of about an order larger than their size. Straight dense periodic chains of identical nano-bumps support TWs that propagate without radiation loss along the chain. The TWs are characterized by wavenumbers that are higher than the SPP wavenumber and, therefore, they are slow waves with respect to both free-space and SPP fields. For wavelength slightly longer than the nano-bump's resonant wavelength the TWs are highly confined to the region near the chain and have a large wavenumber. These TWs can be excited efficiently by a localized source placed near the chain but their propagation length is small due to the increased loss associated with the nano-bump's resonances. For wavelength sufficiently longer than the nano-bump's resonant wavelength, the TWs have a large propagation length with a wavenumber approaching the SPP wavenumber. However, the TWs are not well confined to the region near the chain and are excited less efficiently. For wavelengths shorter than the nano-bump's resonant

wavelength, no TWs are supported. The TWs supported by nano-bump chains were shown to have substantially larger propagation lengths as compared to free-standing chains of the same size and for the same TW field cross-sectional decay rate. This property is important in applications requiring low loss waveguidance.

TWs also are supported by disordered chains. For the chosen structure parameters, chains with disorder in the nano-bump's position support TWs much more efficiently than chains with disorder in the nano-bump's size. The reason is a shift of nano-bump's resonant frequencies with a change of the nano-bumps' size. In addition, the identified TWs can propagate efficiently along chains with sharp bends. Due to strong near-field interactions between the nano-bumps, the transmission through the bend is much stronger in the case of near-resonant rather than off-resonant nano-bumps.

In addition to the ability to support TWs, chains of nano-bumps can be used to manipulate SPPs on the surface. For example, dense chains can reflect SPPs with stronger reflection for frequencies near the nano-bumps' resonant frequency. Sparser chains allowing proper phase matching conditions can lead to phenomena of resonant coupling/radiation between the TWs and incident/scattered SPP or free-space fields.

The chains of nano-particles on metal surface can find uses to construct waveguides and resonators for compactly integrated systems. They also can be used to construct SPP reflectors, splitters, filters, and lasers. Understanding the identified phenomena is an important step towards understanding more general mechanisms including phenomena of cross-coupling between TWs, free-space fields, and SPPs. Such mechanisms are subject to further investigation.

Acknowledgments

This research was supported by AFOSR under MURI grant on electromagnetic simulation of antennas and arrays designed using novel electronic materials and conformal to large complex bodies. The research was partially supported by Nanoscale Interdisciplinary Research Teams (NIRT) program, National Science Foundation (NSF).

#These authors contributed equally to this work.